

Study of Thin Optical Films Properties Using High-performance Atomistic Simulation

Fedor V. Grigoriev¹, Vladimir B. Sulimov¹ , Alexander V. Tikhonravov¹ 

© The Authors 2024. This paper is published with open access at SuperFri.org

Full-atomistic modeling of the deposition of TiO₂, SiO₂ and TiO₂-SiO₂ films is performed using parallel calculations. The dependence of film density on the deposition angle and deposition energy is studied. Simulation of post-deposition annealing of film structures is also carried out. Mechanical stresses in TiO₂-SiO₂ films, arising due to differences in the properties of silicon dioxide and titanium dioxide, are calculated. It is found that the film density decreases with decreasing deposition energy and increasing deposition angle. The use of surfacing annealing leads to an increase in film thickness. In two-layer TiO₂-SiO₂ films, the stresses are compressive. Particular attention is paid to reducing computational costs when simulating large atomistic clusters, consisting of hundreds of thousands of atoms. Reducing the parameter that determines the calculation of the electrostatic part of interatomic energy significantly reduces the simulation time. At the same time, in this case, the accuracy of determining the electrostatic energy in the reciprocal space decreases, which should be taken into account during modeling.

Keywords: thin films structure, simulation of the deposition process, molecular dynamics, silicon dioxide films, titanium dioxide films, high-performance simulation.

Introduction

Multilayer transparent coatings are widely used in optical and optoelectronic devices for various purposes [23–25]. Typically, these coatings consist of several dozen dielectric layers with different refractive indices. The number of layers and their composition are selected taking into account the required properties of the coating.

There are many different ways to make a clear coat. Physical vapor deposition (PVD) is one of the most widely used methods. In PVD, production process is carried out in a vacuum chamber. Atoms extracted from the target by evaporation or sputtering [10] pass through the chamber and are deposited on the substrate. When the thickness of a certain layer is reached, the target changes and the deposition of the next layer begins. The growth process continues until all layers are deposited.

The deposition process and the properties of the growing layers significantly depend on the conditions in the vacuum chamber, such as the temperature of the substrate, the pressure and composition of the atmosphere in the vacuum chamber, the energy and angular distribution of particles arriving from the target to the substrate, and the flux density of these particles [2, 29, 32]. Experimental study of the corresponding dependencies is a difficult task due to the non-equilibrium nature of the growth process and the large number of parameters affecting deposition. For these reasons, mathematical modeling of the process in a vacuum chamber can make a significant contribution to understanding how exactly process parameters affect film properties.

The most fundamental approach to such modeling is the atomistic one, in which the interactions of the atoms involved in the process are explicitly considered. All atomistic methods can be divided into quantum and classical. Quantum methods are more fundamental than the classical ones, but require large computing resources. For this reason, the characteristic sizes of

¹Research Computing Center, Lomonosov Moscow State University, Moscow, Russia

simulated clusters in quantum simulations are limited to approximately a few nanometers. At the same time, important film parameters require modeling on a scale of tens of nanometers. For this reason, only classical atomistic methods are used to simulate the deposition process.

Currently, these methods are widely used for the calculation of structural, mechanical and some optical parameters of the films [14]. In the present work, we focus on the modeling, requiring a lot of computational resources, in particular:

1. Full-atomistic simulation of thin film deposition. Time of the simulation depends on the number of the atoms N in the films as $\sim N^2 \ln N$;
2. Simulation of the structure of the glancing angle deposited (GLAD) films. These films include nanostructures with characteristic dimensions more than several nanometers. The simulation clusters should include at least several nanostructures. For these reasons, the dimensions of these clusters reach tens of nanometers and consist of millions of atoms.
3. Calculation of stresses in the growing films. The value of main components of stress tensors depends noticeably on the films thickness [13] on a scale of at least several tens of nanometers.
4. Simulation of the post-deposition annealing of the film. The study of changes in film parameters as a result of annealing requires long-term modeling.

The most time-consuming part of atomistic modeling involves calculating the energy of interatomic interaction. The composition of optical film-forming materials includes atoms belonging to various chemical elements. Due to differences in ionization potential and electron affinities of different chemical elements, partial charges appear on atoms. The Coulomb interaction of these charges is long-range and requires special techniques to take it into account. One of these techniques is based on the so-called Ewald summation [9], when the total electrostatic energy is represented by two terms.

First of them quickly converges in real space due to the introduction of a factor that decreases exponentially with the interatomic distance. The second term is long-range, but converges quickly in reciprocal (Fourier) space. The computational cost of this method was significantly reduced by using the Particle Mesh Ewald (PME) method [7]. This method uses approach that simplifies the calculation of inverse electrostatic energy. This approach is justified since this term, as a rule, makes a small contribution to the energy of electrostatic interaction. In this work, in addition to the above-mentioned problems of modeling the characteristics of optical films, we also consider the computational cost of parallel modeling with various parameters used in the calculation of electrostatic interactions.

The simulation was performed using the equipment of the shared research facilities of HPC computing resources at Lomonosov Moscow State University [31]. The processors with following characteristics were used: Intel Xeon Gold 6126, 2.6 GHz, 12 cores, 16 GB (queue pascal in the supercomputer Lomonosov-2). The GROMACS program [1] is used for the MD simulation. The VMD [20] program is used for the visual analysis of the atomistic structures of the clusters.

The article is organized as follows. Section 1 is devoted to description of the method of the atomistic simulation of the vapor deposition process. The results of the simulations are discussed in Section 2, including dependence of film density on the simulation parameters (Subsection 2.1), mechanical stresses (Subsection 2.2) and post-deposition annealing (Subsection 2.3). Conclusion summarizes the study.

1. Method of Simulation of Deposition Process

The scheme of the physical vapor deposition (PVD) and simulation area are shown in Fig. 1.

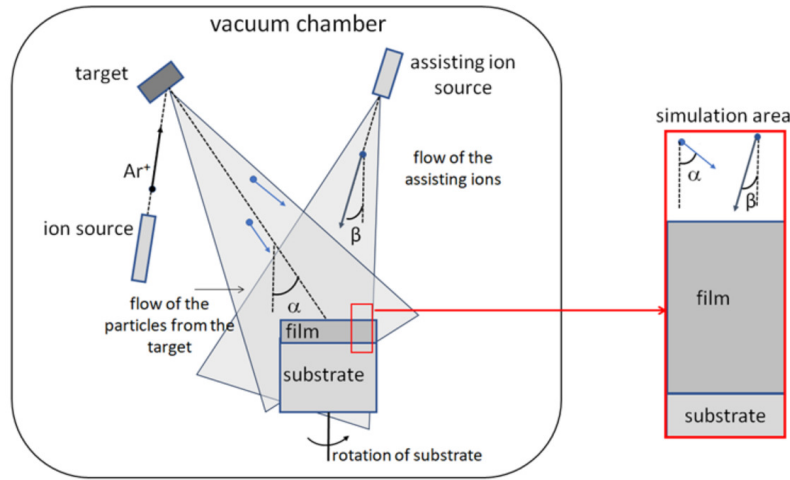


Figure 1. The scheme of the deposition process and simulation area

The particles are sputtered from the target by the high-energy argon ions and are moved to the substrate. The distance between substrate and target is much larger than the dimension of the substrate. Thus, if we neglect the collision of particles with gas molecules, then we can assume that the angles of incidence of the particles on the substrate are the same. The sputtering of the target relate to the high-energy deposition process. In low-energy deposition the particle are emitted due to heating of the target by different methods. In this case, kinetic energy of the particles arriving to the substrate is tenths of an eV. The low-energy deposition, when atoms are extracted from the target by heating, is often accompanied by the ions assisting [19, 34] to improve quality of the growing film (Fig. 1). In this method, the substrate bombard by the high-energy ions, for instance, oxygen ions, that result in the formation of dense and homogeneous film. Substrate rotation is also used to achieve a more homogeneous structure.

The full-atomistic MD simulation is used for the modeling of the final stage of the deposition process, when atoms, extracted from the target, arrive to the substrate, oxidize by the oxygen of the vacuum chamber and form chemical bonds with atoms of film. The macroscopic object – growing film – in the simulation is represented as a microscopic cluster with a characteristic dimension 10–100 nm (Fig. 1, right side). The simulation is organized as a step-by-step procedure [16]. Initially, the substrate structure is prepared using melting-quenching of crystalline SiO_2 cluster [11]. As a result, a cluster of glassy silicon dioxide is formed. The deposition simulation then begins. At each stage, silicon and oxygen atoms are randomly placed at the top of the simulation window. The value of the initial velocities corresponds to the given value of the kinetic energy of the deposited atoms. The directions of the velocities are the same and correspond to the deposition angle. When MD simulation begins, atoms move to the substrate and previously deposited film layers and interact with them, forming chemical bonds. Atoms reflected from the surface are removed after the simulation is completed. The duration of one deposition step is 10 ps. The number of deposition steps depends on the thickness of the film and can reach several thousands.

In the present work, the SiO_2 , TiO_2 and SiO_2 - TiO_2 films are simulated. The potential energy of interatomic interaction for these films is calculated within the DESIL force field [16, 18]:

$$U = \frac{q_i q_j}{r_{ij}} + \frac{A_{ij}}{r_{ij}^{12}} - \frac{B_{ij}}{r_{ij}^6}, \quad (1)$$

where $q_{i(j)}$ is the charge of the $i(j)$ -th atom, $q_O = -0.5q_{Si} = -0.65e$ for silicon dioxide and $q_O = -0.5q_{Ti} = -1.098e$ for titanium dioxide. The parameters of the Lennard-Jones potential are listed in Tab. 1.

Table 1. Parameters A_{ij} and B_{ij} of the Lennard-Jones potential, Eq. (1)

TiO ₂ [19]		
Types of atoms	A_{ij} (kJ · nm ⁶ /mol)	B_{ij} (kJ · nm ¹² /mol)
Ti-Ti	$5.062 \cdot 10^{-4}$	$3.1195 \cdot 10^{-8}$
O(Ti)-O(Ti)	$3.0009 \cdot 10^{-3}$	$1.735775 \cdot 10^{-6}$
Ti-O(Ti)	$1.4368 \cdot 10^{-3}$	$2.90927 \cdot 10^{-7}$
SiO ₂ [17]		
Types of atoms	A_{ij} (kJ · nm ⁶ /mol)	B_{ij} (kJ · nm ¹² /mol)
Si-Si	$5.0 \cdot 10^{-4}$	$1.5 \cdot 10^{-6}$
O(Si)-O(Si)	$5.0 \cdot 10^{-4}$	$1.5 \cdot 10^{-6}$
Si-O(Si)	$4.2 \cdot 10^{-3}$	$4.6 \cdot 10^{-8}$
Ti-Si1	$5.0 \cdot 10^{-4}$	$2.16 \cdot 10^{-8}$

All the atoms in the simulation clusters are taken into account when potential energy of the interaction is calculated. The Berendsen thermostat [6] is applied to keep the simulation box temperature, $T = 300$ K, constant. The time step in the numerical integration of the equation motion is 0.5 fs. The periodic boundary conditions are applied. The simulation in every step is carried out using the NVT (constant number of particles, volume and temperature) ensemble. After each deposition step, the vertical size of the simulated cluster is increased by 0.01 nm to account for the increase in the thickness of the growing film.

Using this scheme, the following technological parameters of the deposition process can be taken into account: angular and energetic distribution of the arriving to the substrate particles, temperature of the substrate, composition of the flow of the particles, angular and energetic distribution of the assisting ions, relative values of the flows of the deposited particles and assisting ions. The duration of the simulation of the deposition process depends on the previously specified final value of film thickness. Upon completion of the simulation, the calculation of the film parameters begins. These parameters are calculated based on the atomistic structure of the deposited cluster.

2. Results and Discussion

In this section, the results of the simulation of the film density, stresses and post-deposition annealing are presented. As it was mentioned in the Introduction, these tasks require a lot of computational resources due to large dimensions of the atomistic clusters. Also, the ways to reduce the simulation time by varying of the parameters of high-performance calculation are studied.

2.1. Thin Films Density

One of the main structural characteristics of the optical film is density. This is explained by the relationship between density and refractive index: an increase in density is accompanied by an increase in the refractive index [30]. The dependence of the density of silicon dioxide and titanium dioxide films on the film thickness is shown in Figures 2, 3 respectively.

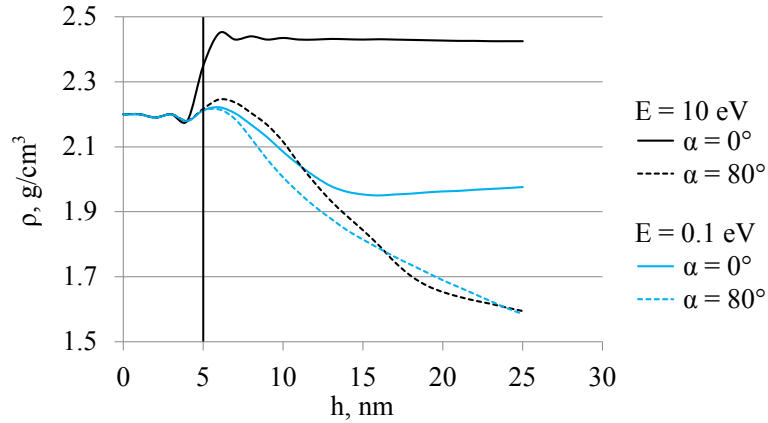


Figure 2. Dependence of the SiO_2 film density (ρ) on the film thickness h , E is the energy of the deposited Si atoms, α is the deposition angle. Vertical solid line denotes the boundary of the substrate

The $\alpha = 0$ corresponds to the normal deposition, when atoms move perpendicular to the substrate. In this case, the film density ρ depends significantly on the energy of the deposition angle. Reduce in the deposition energy results in the noticeable decrease in the film density. The thickness of the transition layer between substrate and film is larger in the case of the low-energy deposition compared to the high-energy deposition. The difference in the ρ at $E = 10$ eV and $E = 0.1$ eV reaches approximately 0.4 g/cm^3 (Fig. 2).

The glancing angle deposition, when the deposited atoms move to the substrate at large deposition angles, results in the formation of the films with low density and high anisotropy [3, 17, 26, 27]. Interestingly, the density of GLAD films depends on the deposition energy much less than the density of normally deposited films (see dotted lines in Fig. 2). The thickness of the transition layer between the substrate and the film is significantly greater than at normal deposition.

Similar trends are observed in the case of titanium dioxide films (Fig. 3). The density shows a significant dependence on the deposition angle and the energy of titanium atoms. Increasing the temperature from 300 K (cold substrate) to 500 K (hot substrate) leads to an increase in the density of low-energy deposited films by approximately 0.1 g/cm^3 .

As it was mentioned in the Introduction section, the time of the simulation of the deposition process is proportional to $t \sim N^2 \ln N$; where N – number of the deposited atoms. The deposition of the clusters, consisting of millions of atoms, requires several days even with using of parallel computations [12]. The parameters PME order and fourierspacing, governing the calculation of the reciprocal part of the electrostatic energy when PME method [7] used in GROMACS program [1], act significantly the simulation time. Reducing the PME order from 8 to 4 reduces the simulation time by more than half. However, such a decrease in time is accompanied by a decrease in the accuracy of the numerical scheme for calculating the inverse part of the electrostatic energy. This decrease acts the calculated parameters of the thin film.

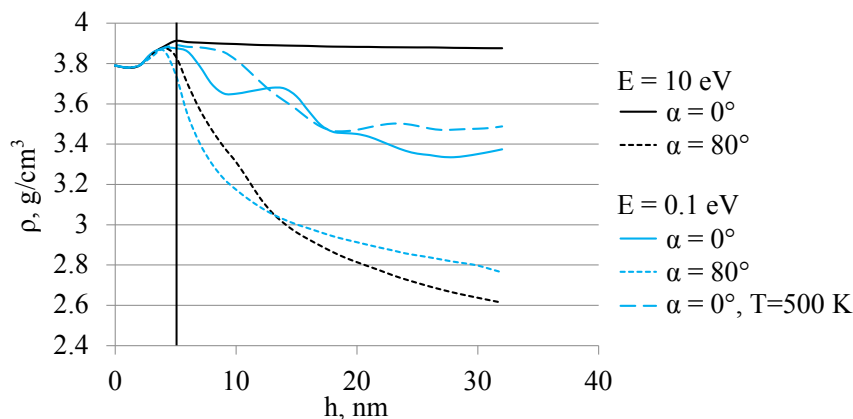


Figure 3. Dependence of the TiO_2 film density (ρ) on the film thickness h , E is the energy of the deposited Ti atoms, α is the deposition angle, T is the substrate temperature, by default $T = 300$ K

The corresponding change in film density is shown in Fig. 4.

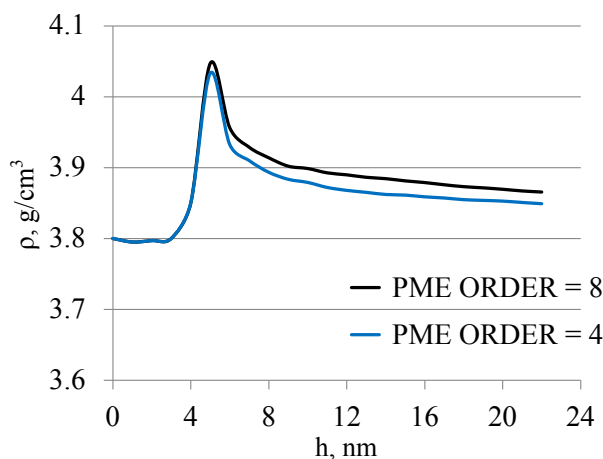


Figure 4. Dependence of the TiO_2 film density (ρ) on the film thickness h at two values of PME order parameter. Energy of the deposited Ti atoms $E(\text{Ti}) = 10$ eV, $T = 300$ K, deposition angle is equal 0

As it can be seen from the graphs, the density calculated for the PME order = 8 exceeds the density for the PME order = 4 by approximately 0.02 g/cm^3 . This value can be considered as an error in calculating the density when the PME order is reduced from 8 to 4. This error is significantly less than the difference in film density for high-energy and low-energy deposition, as well as for normal and grazing deposition angles (Figures 2, 3). Thus, the PME order = 4 variant can be used when studying the dependence of film density on deposition energy and deposition angle.

2.2. Calculation of Stresses

Stresses in the growing films, arising due to differences in the mechanical parameters of the deposited layers of the different composition act significantly characteristics of the transparent coatings [8, 33]. Large stresses can deform coatings leading to difficulties when using them in devices [5]. For this reason, the calculation of the stresses in the growing films is an actual task for the mathematical modeling.

In frame of the full-atomistic MD approach stresses are defined using the pressure tensor, which is calculated using the kinetic energy tensor and the virial tensor [1, 28]. The procedure of the stress calculation in TiO₂–SiO₂ films includes the following steps:

1. Equilibration of the previously deposited TiO₂ layer in the asymmetric NPT (constant number of the particles, pressure and temperature, $T = 300$ K) ensemble during 20 ps. The asymmetric ensemble is required since the pressure in the horizontal and vertical directions differs significantly due to empty space above the TiO₂ layer surface. The duration of 20 ps is enough for the relaxation of the main components of the pressure tensor.
2. Deposition of the SiO₂ layer to TiO₂ layer in NVT (constant number of the particles, volume and temperature, $T = 300$ K) ensemble. Using of this ensemble models the structural restriction to deposited SiO₂ sublayers by TiO₂ layer. These restrictions results in the occurring of the stresses.
3. Every 100 deposition steps, the deposition procedure is interrupted. The deposited structure is simulated in the NVT ensemble for 100 ps, and the main components of the stress tensor are averaged along the trajectory. The deposition process then begins again.

The several structures of TiO₂–SiO₂ films, obtained in this way, are shown in Fig. 5. The cluster of TiO₂ films, deposited at $T = 300$ K and energy of titanium atoms $E(\text{Ti}) = 10$ eV, was obtained in the previous work [18].

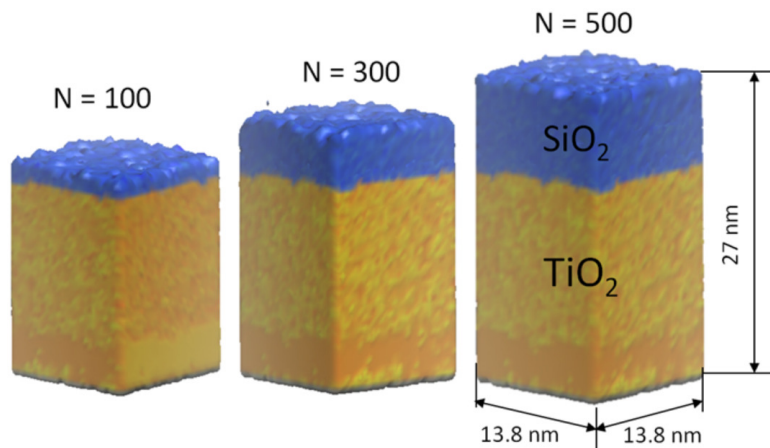


Figure 5. Atomistic clusters of TiO₂–SiO₂ films for different number N of the deposition steps

As it was mentioned in the previous subsection, the value of the PME order parameter significantly decreases the simulation time t (Fig. 6).

In the considered cases, the gain in simulation time is about two and a half times. This gain in t value remains constant over the considered interval of the number of deposition steps N . The second parameter, fourierspacing, also affects the simulation time, but the corresponding effect is less noticeable than for the PME order: increase fourierspacing from 0.12 nm to 0.2 nm leads to a decrease in the t value by approximately 15–20 %.

Results of the calculation of the main component of the stress tensor are shown in Fig. 7.

The all values are negative, that corresponds to the compressive type of the stress. In the case of PME order = 8 the absolute values of σ_{xx} and σ_{yy} are less than in the case of PME order = 4. At PME order = 8 both σ_{xx} and σ_{yy} values decrease at $N > 200$. This tendency is not reproduced at PME order = 4. To summarize, reduce in the PME order value changes significantly the calculated values of the stress tensor components. For this reason, the results

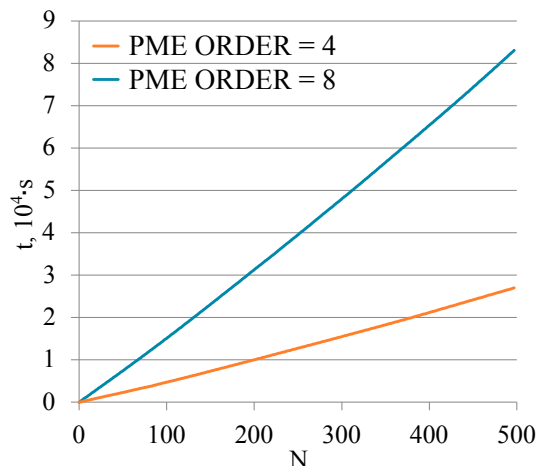


Figure 6. Dependence of the simulation time t on the number of the deposition steps, N at two values of PME order parameters. Number of cores is equal to 32

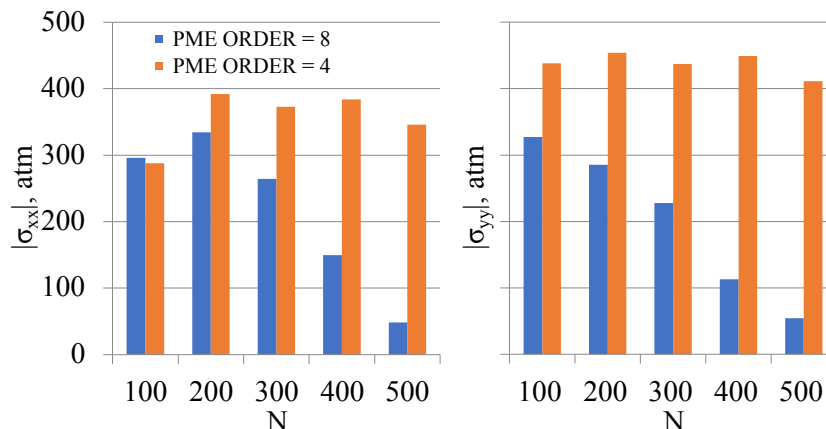


Figure 7. Absolute values of the stress tensor components for two values of the PME order parameter, N is the number of the deposition steps

obtained at PME order = 4 should be considered as preliminary and checked, at least in some points, by calculation at PME order = 8.

2.3. Simulation of Annealing

The post-deposition annealing of the optical coating and film is used to increase their quality and modify the properties [24]. Annealing reduces the refractive index and optical thickness [21], increase the transmittance of the films [22], acts the surface of films, their structural and electrical properties [4].

The annealing can be simulated by full-atomistic simulation. In the agreement with the experiments, the simulation procedure includes the following stages:

1. Heating of the deposited atomistic cluster over time τ from the $T = 300$ K to the annealing temperature T_a .
2. Equilibration of the atomistic cluster at temperature T_a during annealing time τ_a .
3. Cooling from the T_a temperature to the initial temperature $T = 300$ K in time τ .
4. Equilibration of the atomistic cluster at $T = 300$ K during the equilibration time τ_a .

Annealing is performed in the NPT ensemble.

In the present work, the following parameters are chosen: $\tau = 500$ ps, $T_a = 2000$ K, $\tau_a = 1000$ ps. These values are close to those previously used in annealing modeling [15].

The results are shown in Fig. 8.

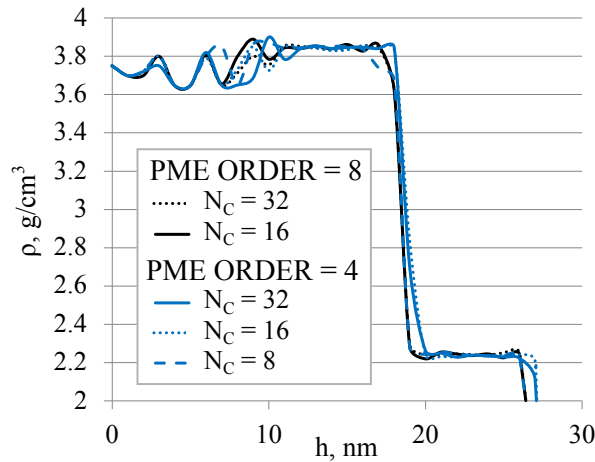


Figure 8. Dependence of the density of the annealed of the in $\text{TiO}_2\text{-SiO}_2$ film on the film thickness at different values of the PME order parameter and different number of the computational cores N_c

Annealing leads to an increase in film thickness. Density fluctuations in the range $h < 12$ nm arise due to the formation of a transition region between the substrate and film. These fluctuations are observed for all values of the PME order parameter and computing cores. The difference in film thickness as the PME order decreases from 8 to 4 reaches approximately 2 nm; see the difference in the position of the film boundary. At the same time, changing the number of computing cores has little effect on the dependence of the film density on h .

The gain in simulation time due to a decrease in the PME order parameter from 8 to 4 times is noticeably greater compared to a similar gain when simulating the deposition process. This can be explained as follows. The simulation of the deposition process is organized as a sequence of steps in which some of the procedures required to run the MD simulation are not parallel. Since the duration of the deposition step is relatively short (10 ps), these procedures have a noticeable impact on the simulation time. In the case of annealing, the procedures are carried out only once and with an annealing simulation duration of 1.5 ns, their impact on the simulation time is negligible.

If the number of computing cores increases by an order of magnitude from 16 to 32, the simulation time is reduced by 1.7 times. A similar gain is obtained in the case of PME order = 4.

Conclusions

Full-atomistic high-performance molecular dynamics simulation of the deposition of TiO_2 , SiO_2 and $\text{TiO}_2\text{-SiO}_2$ films is performed. The films parameters that require the use of large atomistic clusters, consisting of hundreds of thousands of atoms, are calculated.

For both TiO_2 and SiO_2 films, the density decreases with decreasing deposition energy and increasing deposition angle. The stresses in the deposited $\text{TiO}_2\text{-SiO}_2$ films are compressive and reach three hundred bar in absolute value. Annealing leads to an increase in film thickness.

Ways to reduce computational costs are discussed. It is revealed that reducing the PME order parameter, which determines the calculation of electrostatic energy in reciprocal space,

reduces the simulation time. It can be used to calculate the dependence of film density on their thickness. At the same time, when calculating stresses, a decrease in the PME order leads to noticeable changes in the absolute values of the stress tensor components.

Acknowledgements

The work was supported by the Russian Science Foundation (grant No. 23-11-00047).

This paper is distributed under the terms of the Creative Commons Attribution-Non Commercial 3.0 License which permits non-commercial use, reproduction and distribution of the work without further permission provided the original work is properly cited.

References

1. Abraham, M.J., Murtola, T., Schulz, R., *et al*: GROMACS: High performance molecular simulations through multi-level parallelism from laptops to supercomputers. *SoftwareX* 1, 19–25 (2015). <https://doi.org/10.1016/j.softx.2015.06.001>
2. Amirzada, M.R., Tatzel, A., Viereck, V., Hillmer, H.: Surface roughness analysis of SiO₂ for PECVD, PVD and IBD on different substrates. *Applied Nanoscience* 6, 215–222 (2016). <https://doi.org/10.1007/s13204-015-0432-8>
3. Badorreck, H., Steinecke, M., Jensen, L., *et al*: Correlation of structural and optical properties using virtual materials analysis. *Optics Express* 27(16), 22209–22225 (2019). <https://doi.org/10.1364/OE.27.022209>
4. Bakri, A., Sahdan, M.Z., Adriyanto, F., *et al*: Effect of annealing temperature of titanium dioxide thin films on structural and electrical properties. In: *AIP conference proceedings*. vol. 1788. AIP Publishing (2017). <https://doi.org/10.1063/1.4968283>
5. Begou, T., Lumeau, J.: Accurate analysis of mechanical stress in dielectric multilayers. *Optics Letters* 42(16), 3217–3220 (2017). <https://doi.org/10.1364/OL.42.003217>
6. Berendsen, H.J., Postma, J.v., Van Gunsteren, W.F., *et al*: Molecular dynamics with coupling to an external bath. *The Journal of chemical physics* 81(8), 3684–3690 (1984). <https://doi.org/10.1063/1.448118>
7. Darden, T., York, D., Pedersen, L.: Particle mesh Ewald: An $N \cdot \log(N)$ method for Ewald sums in large systems. *The Journal of chemical physics* 98(12), 10089–10092 (1993). <https://doi.org/10.1063/1.464397>
8. Ennos, A.E.: Stresses developed in optical film coatings. *Applied optics* 5(1), 51–61 (1966). <https://doi.org/10.1364/AO.5.000051>
9. Ewald, P.P.: Die berechnung optischer und elektrostatischer gitterpotentiale. *Annalen der physik* 369(3), 253–287 (1921). <https://doi.org/10.1002/andp.19213690304>
10. Greene, J.E.: Tracing the recorded history of thin-film sputter deposition: From the 1800s to 2017. *Journal of Vacuum Science & Technology A* 35(5) (2017). <https://doi.org/10.1116/1.4998940>

11. Grigoriev, F., Sulimov, A., Kochikov, I., *et al*: Computational experiments on atomistic modeling of thin-film deposition. *Applied Optics* 56(4), C87–C90 (2017). <https://doi.org/10.1364/AO.56.000C87>
12. Grigoriev, F., Sulimov, V., Tikhonravov, A.: High-performance full-atomistic simulation of optical thin films. *Supercomputing Frontiers and Innovations* 5(3), 130–133 (2018). <https://doi.org/10.14529/jsfi180325>
13. Grigoriev, F.V., Sulimov, V.B., Tikhonravov, A.V.: Atomistic simulation of stresses in growing silicon dioxide films. *Coatings* 10(3), 220 (2020). <https://doi.org/10.3390/coatings10030220>
14. Grigoriev, F.V., Sulimov, V.B.: Atomistic simulation of physical vapor deposition of optical thin films. *Nanomaterials* 13(11), 1717 (2023). <https://doi.org/10.3390/nano13111717>
15. Grigoriev, F., Katkova, E., Sulimov, A., Sulimov, V., Tikhonravov, A.: Annealing of deposited SiO₂ thin films: full-atomistic simulation results. *Optical Materials Express* 6(12), 3960–3966 (2016). <https://doi.org/10.1364/OME.6.003960>
16. Grigoriev, F., Sulimov, A., Kochikov, I., *et al*: Supercomputer modeling of the ion beam sputtering process: full-atomistic level. In: *Optical Systems Design 2015: Advances in Optical Thin Films V*. vol. 9627, pp. 34–42. SPIE (2015). <https://doi.org/10.1117/12.2190938>
17. Grigoriev, F., Sulimov, V., Tikhonravov, A.: Structure of highly porous silicon dioxide thin film: Results of atomistic simulation. *Coatings* 9(9), 568 (2019). <https://doi.org/10.3390/coatings9090568>
18. Grigoriev, F., Sulimov, V., Tikhonravov, A.: Application of a large-scale molecular dynamics approach to modelling the deposition of TiO₂ thin films. *Computational Materials Science* 188, 110202 (2021). <https://doi.org/10.1016/j.commatsci.2020.110202>
19. Guo, C., Kong, M.: Fabrication of ultralow stress TiO₂/SiO₂ optical coatings by plasma ion-assisted deposition. *Coatings* 10(8), 720 (2020). <https://doi.org/10.3390/coatings10080720>
20. Humphrey, W., Dalke, A., Schulten, K.: Vmd: visual molecular dynamics. *Journal of molecular graphics* 14(1), 33–38 (1996). [https://doi.org/10.1016/0263-7855\(96\)00018-5](https://doi.org/10.1016/0263-7855(96)00018-5)
21. Jiang, Y., Ji, Y., Liu, H., *et al*: Insights into effects of thermal annealing on optical properties of SiO₂ films. In: *6th International Symposium on Advanced Optical Manufacturing and Testing Technologies: Advanced Optical Manufacturing Technologies*. vol. 8416, pp. 106–110. SPIE (2012). <https://doi.org/10.1117/12.974980>
22. Li, S., Liu, C., Zhu, T., *et al*: Effects of the thermal treatments on the optical properties of SiO₂ anti-reflective coatings on sapphire windows. *Infrared Physics & Technology* 137, 105151 (2024). <https://doi.org/10.1016/j.infrared.2024.105151>
23. Martinu, L., Poitras, D.: Plasma deposition of optical films and coatings: A review. *Journal of Vacuum Science & Technology A: Vacuum, Surfaces, and Films* 18(6), 2619–2645 (2000). <https://doi.org/10.1116/1.1314395>

24. Piegari, A.: FF (Ed.) *Optical Thin Films and Coatings* (2018)
25. Schulz, U.: Review of modern techniques to generate antireflective properties on thermoplastic polymers. *Applied optics* 45(7), 1608–1618 (2006). <https://doi.org/10.1364/AO.45.001608>
26. Smy, T., Vick, D., Brett, M., *et al*: Three-dimensional simulation of film microstructure produced by glancing angle deposition. *Journal of Vacuum Science & Technology A: Vacuum, Surfaces, and Films* 18(5), 2507–2512 (2000). <https://doi.org/10.1116/1.1286394>
27. Tait, R., Smy, T., Brett, M.: Modelling and characterization of columnar growth in evaporated films. *Thin Solid Films* 226(2), 196–201 (1993). [https://doi.org/10.1016/0040-6090\(93\)90378-3](https://doi.org/10.1016/0040-6090(93)90378-3)
28. Thompson, A.P., Plimpton, S.J., Mattson, W.: General formulation of pressure and stress tensor for arbitrary many-body interaction potentials under periodic boundary conditions. *The Journal of chemical physics* 131(15) (2009). <https://doi.org/10.1063/1.3245303>
29. Tolenis, T., Grinevičiūtė, L., Smalakys, L., *et al*: Next generation highly resistant mirrors featuring all-silica layers. *Scientific reports* 7(1), 10898 (2017). <https://doi.org/10.1038/s41598-017-11275-0>
30. Vedam, K., Limsuwan, P.: Piezo-and elasto-optic properties of liquids under high pressure. II. Refractive index vs density. *The Journal of Chemical Physics* 69(11), 4772–4778 (1978). <https://doi.org/10.1063/1.436530>
31. Voevodin, V.V., Antonov, A.S., Nikitenko, D.A., *et al*: Supercomputer Lomonosov-2: Large scale, deep monitoring and fine analytics for the user community. *Supercomputing Frontiers and Innovations* 6(2), 4–11 (2019). <https://doi.org/10.14529/jsfi190201>
32. Xu, C., Qiang, Y., Zhu, Y., *et al*: Effects of deposition parameters on laser-induced damage threshold of Ta₂O₅ films. *Optics & Laser Technology* 42(3), 497–502 (2010). <https://doi.org/10.1016/j.optlastec.2009.09.004>
33. Ying, D., Zhong, T.: Effects of thickness and annealing on the residual stress of TiO₂ film. *Optics Continuum* 3(3), 287–295 (2024). <https://doi.org/10.1364/OPTCON.506007>
34. Zoeller, A., Beisswenger, S., Goetzelmann, R., Matl, K.: Plasma-ion-assisted-deposition: a novel technique for the production of optical coatings. In: *Optical Interference Coatings*. vol. 2253, pp. 394–402. SPIE (1994). <https://doi.org/10.1117/12.192112>